CICE 2023 Rio de Janeiro – Brazil 11TH INTERNATIONAL CONFERENCE ON FRP COMPOSITES IN CIVIL ENGINEERING

NUMERICAL SIMULATION OF LAP-SHEAR AND PRESTRESS FORCE RELEASE TESTS OF FRP STRIPS GLUED ON CONCRETE: CONSIDERATIONS ABOUT THE ROLE OF MIXED-MODE FRACTURE PROCESSES

Enzo Martinelli, University of Salenro, Italy, e.martinelli@unisa.it
Matteo Breveglieri, Empa, Switzerland, matteo.breveglieri@empa.ch
Niloufar Moshiri, Mageba, Switzerland, nilou.msh@gmail.com
Christoph Czaderski, Empa, Switzerland, christoph.czaderski@empa.ch

ABSTRACT
Lap-shear tests carried out on Externally Bonded (EB) FRP strips or, more recently, prestress force-release tests have established in the scientific community as experimental methods intended at determining the actual bearing capacity of EB FRP strips glued to concrete. The results of these tests are employed to scrutinize the interface behavior between FRP and supporting materials, which is generally modelled as a pure mode II fracture process. This paper shows the results of a numerical study intended at further unveiling the role of mixed-mode fracture parameters in the debonding process between FRP strips and concrete in lap-shear and prestress force releasing tests.

KEYWORDS
Concrete, Debonding, Mixed mode

INTRODUCTION
Existing reinforced concrete (RC) structures are often in need for strengthening due to either ageing of materials, damage induced by service life actions or flaws in the original design and realization (Biondini & Frangopol, 2016). Strengthening techniques based on utilising Fiber-Reinforced Polymer (FRP) composite systems have been gaining general consensus across the last two decades and are nowadays established as a competitive technical solution in several conditions (Meier et al., 2016). More specifically, the use of Externally Bonded (EB) FRP strips glued to RC members with the aim to enhance their strength is a widely adopted solution both in buildings and in bridges (Czaderski & Motavalli, 2007).
However, the resulting effectiveness of strengthening interventions based on the use of FRP in RC structures is often controlled by the FRP-to-concrete interface behaviour, as the so-called “debonding” failure often occurs earlier than the FRP strip can actually develop all its tensile strength (Breveglieri et al., 2018). Therefore, since the beginning of research activities in composites for construction, people have paid a great attention to the phenomenological aspects related to debonding failure, its possibly different initiation points in FRP strengthening tested in bending and the complex mechanical processes that stand behind those empirical observation (Teng et al., 2002).
As a general point, it should be noticed that the wide majority of mechanical models available in the scientific literature, including those which are the bases of the current code provisions, assume that debonding is a fracture process, which develops in pure mode II (Caggiano et al., 2013). This assumption has been widely accepted and allows understanding the main features of the debonding process for FRP strips EB to concrete (or other quasi-brittle material) substrates, as it leads to simplified expressions for the maximum load that can be transferred by the FRP-to-concrete joint under consideration and the distribution of relative displacements (slips) and bond stresses throughout the adhesive interface (Martinelli, 2021).
However, experimental observations and mechanical considerations show that the excentricity between the axial stresses arising within the FRP strip cross section and the bond stresses distributed beneath it, should result in a bending action on the strip itself, which leads to both out of plane relative

displacements with respect to the interface plane and normal (peeling) stresses throughout the adhesive interface (De Lorenzis & Zavarise, 2008).
Allthough some early analytical solutions developed for steel plates epoxy-glued to concrete (according to the so-called *béton plaque* technique) showed that an elastic distribution of peeling stresses can be determined by assuming a beam on Winkler soil scheme, more recent developments have tried to go deeper into the investigation of actual distribution of shear and peeling stresses throughtout the interface at various stages of the fracture process that leads to peeling (Roberts, 1989). Specifically, the authors have already proposed a numerical procedure based on an uncoupled formulation for shear and peeling stresses (and, correspondingly, relative axial and normal displacements) (Martinelli et al, 2011).
The present paper is a further development of that past model as it assumes a fully coupled formulation for the mixed-mode fracture process. Specifically, the formulation is based on the flow theory of plasticity including softening as a result of the fracture process controlled by two independent values of fracture energy for the two ideal modes I and II (Carol et al., 1997). Specifically, zero-thickness interface elements are derived with the aim to connect the FRP strip and the concrete substrate. Furthermore, the present formulation ideally covers both the case of lap-shear and stress-release tests, the latter being realised by gluing an initially prestressed strip which is then released from one side, possibly up to debonding of the interface (Moshiri et al, 2023).
That said, the paper is structured as follows. Section 2 proposes the mathematical formulation of the mechanical model and its numerical solution based on the finite element method. Section 3 summarises the results of some experimental tests carried out on FRP strips glued to concrete according to the Externally Bonded Reinforcement On Grooves (EBROG) technique (Moshiri et al., 2023). Both the case of a lap-shear test of (non prestressed FRP strips) and the one of a stress-release test are considered herein. Section 4 shows the comparisons between experimental results and numerical simulation with the aim to show the potential of the present model to simulate debonding phenomena of FRP strips EB to concrete. Section 5 summarises the main findings of this study, show some limitations of the current formulation and figures out some of the possible future developments.

MODEL FORMULATION

The present numerical model is based on the following assumptions:

- the FRP strip behaves elastically and is modelled according to the Bernoulli beam;
- the concrete substrate is rigid;
- the epoxy adhesive layer is modelled in plane-strain elasticity;
- the connection between the epoxy layer and the concrete substrate is modelled via a zero-thickness layer where mixed mode fracture develops according to the flow theory of plasticity with softening (Carol et al., 1997).

In principle, the numerical model is meant to simulate the behaviour of FRP strips glued to concrete, either prestressed or not, and subjected to the load conditions realised in either prestress-release (Figure 1b) and lap-shear (1a) tests. However, the present formulation and the corresponding validation is limited to the case of FRP strips subjected to lap-shear tests.

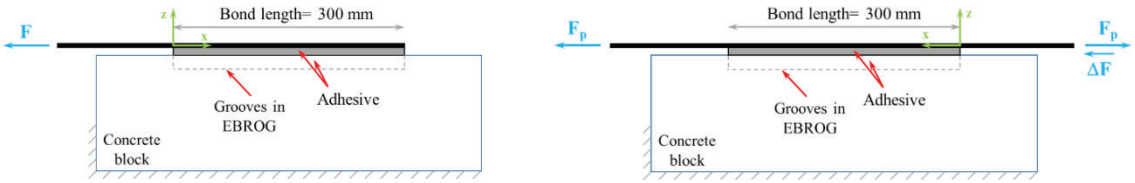

a) Lap-shear test b) Prestress-release test

Figure 1: Layout examples of possible tests on FRP strips glued to concrete

The mechanical assumptions of the model can easily lead to the fundamental equations for the present model, which is formulated in a 2D context as represented in Figure 3. Thus, each node is associated with the three usual degrees of freedom u, v and φ.
The possible prestressing affects the axial response of the beam, as the compatibility equation between axial displecements u and total axial strains ε can be described as follows:

$$\boldsymbol{\Delta\sigma} = \boldsymbol{K}_{el} \cdot \boldsymbol{\Delta u}^{el} \qquad \text{Eq. 1}$$

Therefore, special emphasis should be placed upon the description of the fracture process via the aforementioned zero-thickness elements, whose linear response can be represented by means of the elastic matrix $\boldsymbol{K}_{el}$:

$$\boldsymbol{\Delta\sigma} = \boldsymbol{K}_{el} \cdot \boldsymbol{\Delta u}^{el} \qquad \begin{bmatrix} \Delta\sigma_N \\ \Delta\sigma_T \end{bmatrix} = \begin{bmatrix} k_N & 0 \\ 0 & k_T \end{bmatrix} \cdot \begin{bmatrix} \Delta u_N^{el} \\ \Delta u_T^{el} \end{bmatrix} \qquad \text{Eq. 2}$$

which relates the generic stress increment $\boldsymbol{\Delta\sigma}$ at each node to the corresponding elastic displacement increment $\boldsymbol{\Delta u}^{el}$, the latter being, in turn, one of the two parts of the total displacement increment $\boldsymbol{\Delta u}$ (consisting of the two vectorial components in the normal *"N"* and tangential *"T"* directions):

$$\boldsymbol{\Delta u} = \boldsymbol{\Delta u}^{el} + \boldsymbol{\Delta u}^{cr} = \begin{bmatrix} \Delta u_N^{el} \\ \Delta u_T^{el} \end{bmatrix} + \begin{bmatrix} \Delta u_N^{cr} \\ \Delta u_T^{cr} \end{bmatrix} \qquad \text{Eq. 3}$$

where $\boldsymbol{\Delta u}^{cr}$ is the cracking displacement increment.
The cracking phenomenon is assumed to begin at a certain point as the corresponding stress state $\boldsymbol{\sigma}=[\sigma_N,\sigma_T]^T$ reaches a "cracking surface" described by the following equation (Figure 2):

$$\boldsymbol{F}(\boldsymbol{\sigma},\boldsymbol{q}) = \sigma_T^{\,2} - \left(c - \sigma_N \tan\phi\right)^2 + \left(c - \chi \tan\phi\right)^2 = 0 \qquad \text{Eq. 4}$$

where $\boldsymbol{q}=(\chi,c,\tan\phi)$.

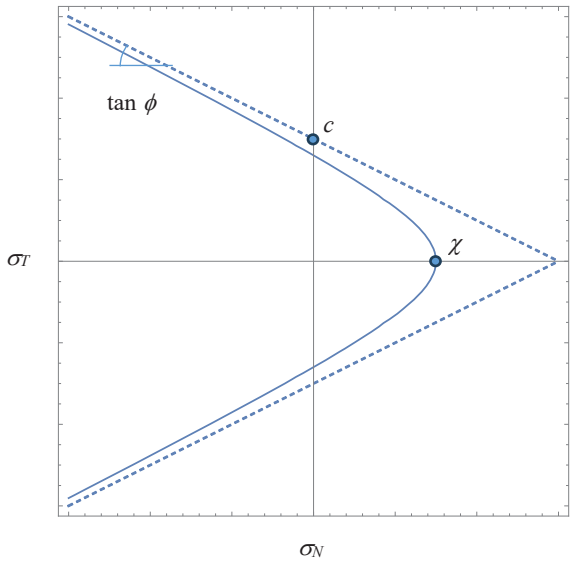

Figure 2: General shape of the cracking surface

The work spent in the fracture process can be evaluated as follows

$$\Delta W^{cr} = \begin{cases} \sigma_N \Delta_N^{cr} + \sigma_T \Delta_T^{cr} & if \quad \sigma_N \geq 0 \\ \sigma_T \Delta_T^{cr} \cdot \left(1 + \dfrac{\sigma_N \tan\phi}{|\sigma_T|}\right) & if \quad \sigma_N < 0 \end{cases} \qquad \text{Eq. 5}$$

where the second expression takes into account the possible contribution of friction in the case of compressive normal stresses. A non-associated "flow" rule relates the cracking displacement increment $\Delta \boldsymbol{u}^{cr}$ and the current stress state:

$$\Delta \boldsymbol{u}^{cr} = \Delta\lambda \cdot \boldsymbol{m} \qquad \text{Eq. 6}$$

where $\Delta\lambda$ is the increment of the cracking multiplier and the vector M can be expressed as follows:

$$\boldsymbol{m} = \boldsymbol{A} \cdot \boldsymbol{n} \qquad with \qquad \boldsymbol{n} = \begin{bmatrix} \frac{\partial F}{\partial \sigma_N} & \frac{\partial F}{\partial \sigma_T} \end{bmatrix}^T \qquad and \qquad \boldsymbol{A} = \begin{bmatrix} f_\sigma^{dil} f_c^{dil} & 0 \\ 0 & 1 \end{bmatrix}. \qquad \text{Eq. 7}$$

The terms f_σ^{dil} and f_c^{dil} are equal to 1 if $\sigma_N > \sigma_{N,dil}$ and vanish as compressions are higher than the latter, which realises the non-associate flow in the fractire process.
The softening behaviour of the farcture process is regulated by the following degradation function:

$$S(\xi) = \frac{e^{-\alpha}\xi}{1 + (e^{-\alpha} - 1)\xi} \qquad \text{Eq. 8}$$

which multiplies the $\boldsymbol{q}$ parameters in Eq. (4) as the fracture process develops, which is regulated by the ratio:

$$\xi_* = \frac{W^{cr}}{G_{F*}} \qquad \text{Eq. 9}$$

where fracture energy in mode I, $G_{F,I}$, is considered for the cohesion term c, and fracture energy in (asymptotic) mode II, $G_{F,II}$, is taken into account for both χ and $tan\phi$.
Therefore, by combining Eq. (2) and (3), the following relationship can be obtained between the increment of both cracking increment $\Delta \boldsymbol{u}$, fracture multiplier $\Delta\lambda$, and the corresponding stress increment $\Delta \boldsymbol{\sigma}$:

$$\Delta \boldsymbol{\sigma} = \boldsymbol{K}_{el} \cdot \left[\Delta \boldsymbol{u} - \Delta\lambda \cdot \boldsymbol{A} \cdot \boldsymbol{n} \right] \qquad \text{Eq. 10}$$

Therefore, the definition of a "consistent" tangent stiffness matrix can be obtained by properly combining Eq. 4 and Eq. 10:

$$\boldsymbol{K} = \boldsymbol{K}_{el} - \frac{\boldsymbol{K}_{el} \cdot \left[\frac{\partial Q}{\partial \boldsymbol{\sigma}} \right]^T \cdot \left[\frac{\partial F}{\partial \boldsymbol{\sigma}} \right] \cdot \boldsymbol{K}_{el}}{H + \frac{\partial F}{\partial \boldsymbol{\sigma}} \cdot \boldsymbol{K}_{el} \cdot \left[\frac{\partial Q}{\partial \boldsymbol{\sigma}} \right]^T} \qquad \text{Eq. 11}$$

where H is the is the hardening/softening parameter:

$$H = -\left[\frac{\partial F}{\partial \boldsymbol{q}} \right]^T \frac{\partial \boldsymbol{q}}{\partial W^{cr}} \frac{\partial W^{cr}}{\partial \boldsymbol{u}^{cr}} \left[\frac{\partial Q}{\partial \boldsymbol{\sigma}} \right]^T \qquad \text{Eq. 12}$$

and $Q(\boldsymbol{\sigma}, \boldsymbol{q}, \boldsymbol{\alpha})$=0 is the so-called "plastic potential" with a collecting the evolution parameters α of Eq. 8 concerning the properties collected within the $\boldsymbol{A}$ matrix in Eq. 7, and

$$\frac{\partial Q}{\partial \boldsymbol{\sigma}} = \boldsymbol{m} \ . \qquad \text{Eq. 13}$$

Further details on the mathematical derivation of Eqs. 11 and 12 and on the mechanical meaning of the obtained quantities are omitted herein for the sake of brevity and can be found in Carol et al (1997).
The solution of the system of nonlinear equations resulting by combining Eq. 4 and Eq. 10 can be obtained via alternative iterative numerical methods (Carol et al, 1997; Caballero et al, 2007).
In the present paper, the model is implemented into 2-node zero-thickness interface elements connecting the adhesive layer with the (rigid) concrete substrate. Therefore, the model consists of (Figure 3):

- *n* Berboulli beam elements representing the FRP strip;
- *n* quadrilateral elastic elements representing the adhesive layer;
- *n+1* 2-nodes zero-thickness elements where both the elastic and cracking response of the FRP-to-concrete interface is lumped.

Therefore, the model consists of *3(n+1)* nodes, each one of which is generally characterised by *3* degrees of freedom (DoF), as the problem is formulated in 2D. More specifically, the FRP strip is modelled as already proposed by the authors in a previous work of theirs (Martinelli et al, 2011). The main difference between that model and the present one are highlighted below:

- the present numerical implementation of the model is based on an Matlab® code (The MathWorks Inc., 2022) entirely coded by the authors and based on an incremental-iterative procedure in displacement control;
- the beam elements representing the FRP strip are connected to an adhesive layer of thickness t_a, characterised by a Young's Modulus E_a and a Poisson's ratio ν_a represented by 4-node plane strain elements;
- the adhesive layer is, in turn connected to zero-thickness elements where all the non linear features of the cracking phenomenon are concentrated.
- the formulation of the complete incremental-iterative procedure implemented to simulate the debonding phenomenon is run in displacement control;
- for each imposed displacement increment, a recursive solution scheme is adopted to solve Eq. 4 and Eq. 10 for each zero-thickness element, whose $\boldsymbol{q}$ parameters are updated after convergence is reached and before proceeding with the subsequent displacement increment;
- at convergence for the current displacement increment (which is achieved as in two subsequent iterations the global response variation is below a given threshold defined in terms of displacements), a further increment is applied at the displacement controlled node.

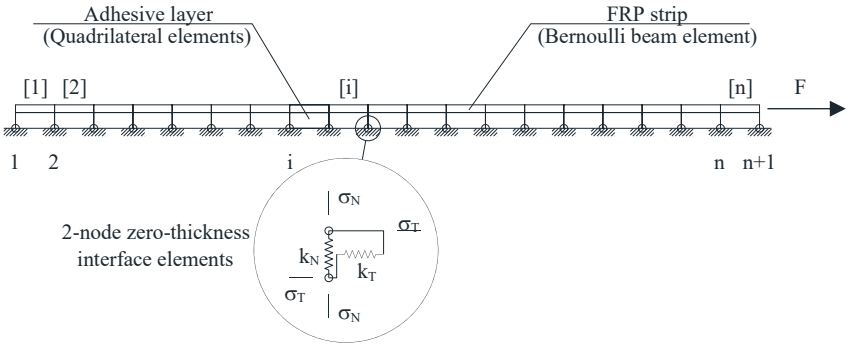

Figure 3: Graphical sketch of the main features of the present numerical model

OUTLINE OF TWO LAP-SHEAR TESTS

The model formulated in this paper is validated by considering the results of two lap-shear tests carried out on two different FRP strips specimens realised according to either the Externally-Bonded Reinforcement (EBR) or the Externally-Bonded Reinforcement on Grooves (EBROG) techniques (Figure 4). The consideration of these two different specimens is intended at emphasising the different values assumed in EBR and EBROG systems by the parameters describing the fracture process (especially the three quantities collected in the vector $\boldsymbol{q}$ of Eq. 4). Besides the inherent difference between the two connection systems, the main geometric properties are common for the two specimens. In fact, in both cases, the FRP strip is b_f=100 mm wide and t_f=1.4 mm thick. Moreover, the bonded length is L=300 mm.

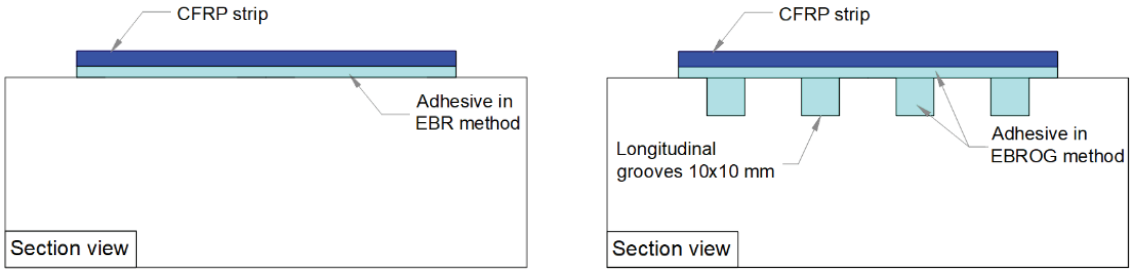

a) EBR interface b) EBROG interface

Figure 4: EBR. Vs EBROG. Techniques for FRP strip connection to concrete

The experimental results obtained from lap-shear tests on EBR-FRP specimens are summarised by Figure 5 and Figure 6. Specifically, Figure 5 shows the observed relationship between the applied lap-shear force and the resulting interface slip at the loaded end of the bonded length.

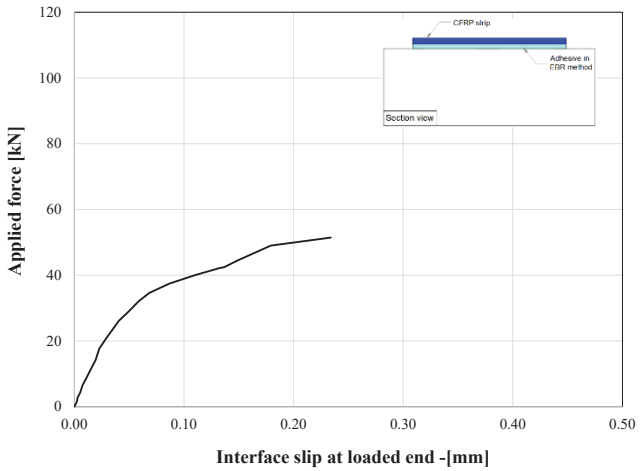

Figure 5: Lap-shear test on EBR-FRP strip: force-displacement response

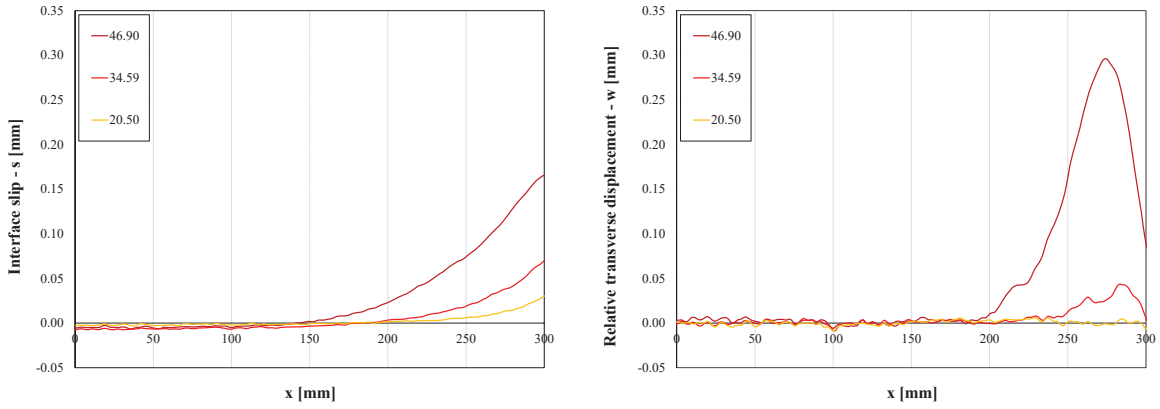

a) Interface slips b) Relative transverse displacements

Figure 6: Lap-shear test on EBR-FRP strip: interface slips and relative transverse displacements

Moreover, Figure 6 depicts the distribution of both interface slips s and relative transverse (out-of-plane) displacements observed throughout the bonded length at three different load levels: the first one (20.56 kN) at the end of the quasi-linear branch that can be observed in Figure 5, the third one (46.90 kN) is close to the full debonding condition and the second one (34.59 kN) is intermediate between the other two. Therefore, the plotted experimental results correspond to different development levels of the debonding phenomenon and, hence, different levels of nonlinearity in the mechanical response of the tested specimens. Figure 7 and Figure 8 show the corresponding experimental results obtained from the lap-shear tests on EBROG-FRP specimens.

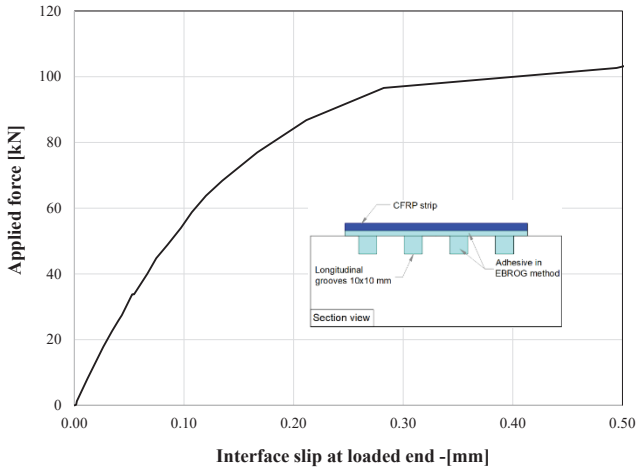

Figure 7: Lap-shear test on EBROG-FRP strip: force-displacement response

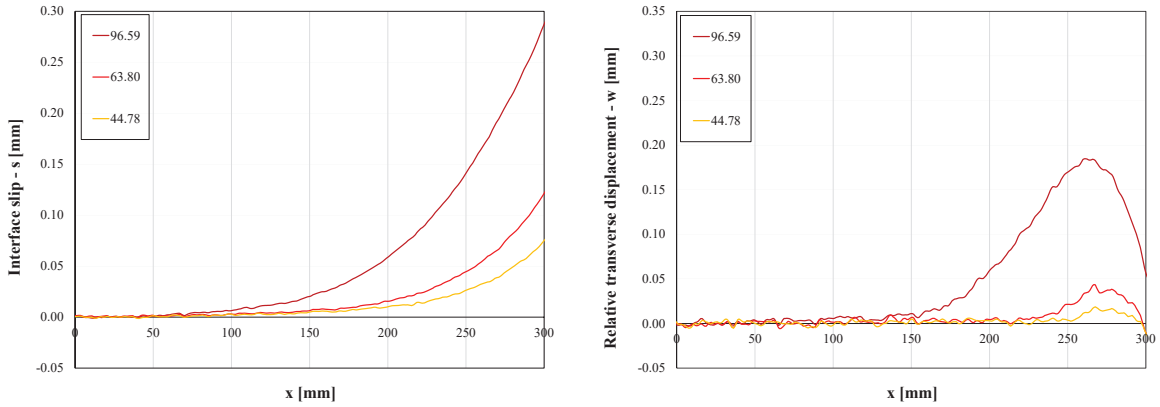

a) Interface slips b) Relative transverse displacements

Figure 8: Lap-shear test on EBROG-FRP strip: interface slips and relative transverse displacements

A comparison between Figure 5 and Figure 7 shows the superior load bearing capacity of the EBROG system with respect to the standard EBR solution. Although the initial stiffness of the two force-slip curves is similar, the EBROG system is characterized by a strength that is almost twice than the one observed in EBR systems and also the displacement capacity is significantly magnified by the presence of a more articulated interface in the EBROG system (Moshiri et al, 2023).

ANALYSIS AND RESULTS

After a sensitivity analysis intended at understanding the relationship between the number of nodes and elements, the resulting accuracy and related computational times, a mesh consisting of n=60 elements for both the FRP strip and the adhesive layer (and, hence, a total of 183 nodes) was considered for the present work. However, already in the current numerical implementation it can be employed with the aim to scrutinise the development of the cracking phenomena that lead the tested specimens to debonding.

The EBR FRP strip has been simulated by assuming the following values for the main mechanical properties $G_{F,I}$=0.20 N/mm and $G_{F,II}$=0.80 N/mm. All the α parameters involved in Eq. 8 are set to zero, which means that a linear evolution of the fracture surface parameters is currently assumed. Figure 9 represents the distribution of both interface slips and relative transverse displacements throughout the bonded length and for different load levels. The two graph show a reasonable agreement in terms of slips, whereas the approximation of the transverse displacement is satisfactory only for the first two considered load levels.

Figure 10 show the evolution of the $W_{cr}/G_{F,I}$ ratio in some specific nodes (Figure 3) and demonstrate that debonding initiate at node n-1, where it develops with a significant mode I component,

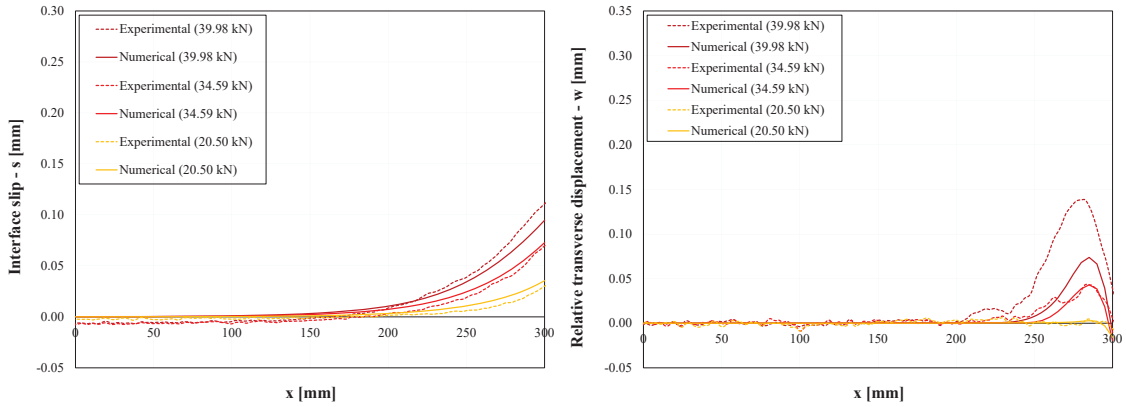

a) Interface slips b) Relative transverse displacements

Figure 9: Numerical vs. Experimental comparison: displacement fields throughout the bonded length (EBR-FRP strip)

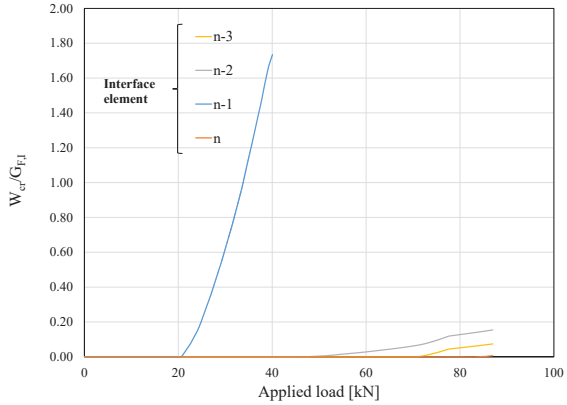

Figure 10: Evolution of the fracture work in some monitored nodes (EBR-FRP strip)

The mechanical behaviour of the EBROG specimen submitted to lap-shear test (Figure 4b) can be simulated with the aim to understand the evolution of the displacement fields throughout the bonded length. Specifically, the EBROG FRP strip has been simulated by assuming the following values for the main mechanical properties $G_{F,I}$=0.70 N/mm and $G_{F,II}$=2.20 N/mm. Like in the case of the EBR FRP strip, all the α parameters involved in Eq. 8 are set to zero, which means that a linear evolution of the fracture surface parameters is currently assumed. Figure 11a) shows that the numerical approximation of the interface slip distribution is reasonably accurate at the three considered load levels, whereas the model – in the present calibration – can only catch the maximum out-of-plane displacements, yet determining a limited extension of the distribution determined through the numerical simulation.

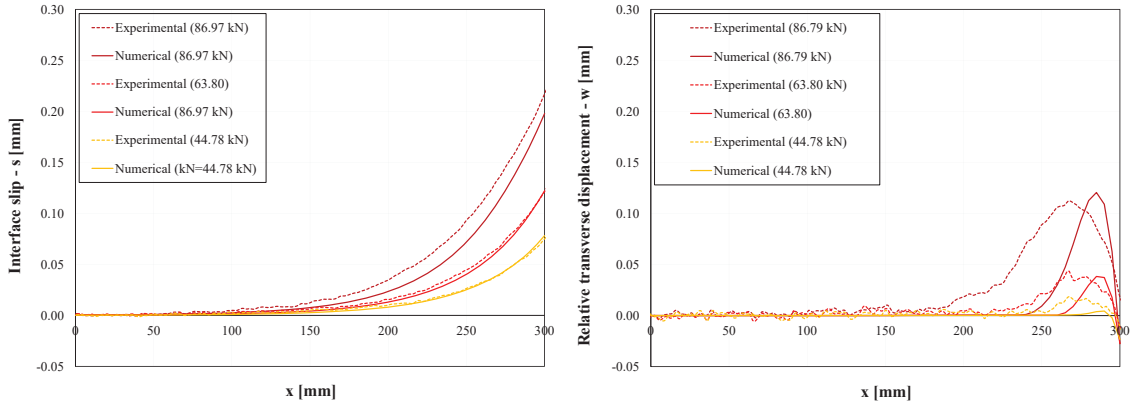

a) Interface slips b) Relative transverse displacements

Figure 11: Numerical vs. Experimental comparison: displacement fields throughout the bonded length (EBROG-FRP strip)

Moreover, like in the case of the EBR specimen, Figure 12 shows that debonding does not begins at the very end of the of the bonded length, but from a more internal one (nodes *n-1* and *n-2*), where shear and normal stresses combine in the most unfavourable way and result in triggering the cracking phenomenon and controlling the whole debonding process.

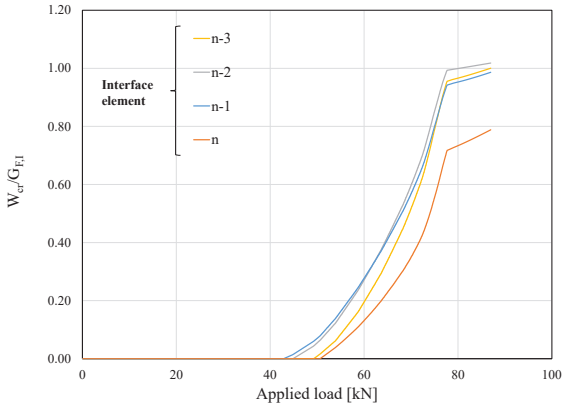

Figure 12: Evolution of the fracture work in some monitored nodes (EBROG-FRP strip)

CONCLUDING REMARKS

The present paper reports the formulation of a novel theoretical model intended at simulating the debonding phenomenon generally occurring in FRP strips glued on a quasi-brittle substrate material, like concrete. Specifically, the model aims at simulating the mixed-mode fracture process developing at the interface throughout the FRP-to-concrete interface, as it is observed from both lap-shear or stress-release tests. The model is formulated by modelling the FRP strip with beam-like elements and assuming plane strain conditions for the adhesive layer. Moreover, all the nonlinear behaviour is lumped within zero-thickness interface elements, which are intended at simulating both the elastic and inelastic response of the adhesive-to-concrete interface. In principle, a proper calibration of the various parameters defining both the elastic springs, the fracture surface and the plastic potential of the model allows for simulating the different behaviour that characterise two different connection solutions, such as EBR and EBROG techniques.

Although the proposed model is characterised by a more sophisticated mechanical formulation and require more computationally challenging numerical solution algorithms, it allows to highlight peculiar aspects of the debonding phenomenon (like the actual initiation of the cracking process and its evolution in mixed mode) which cannot be caught by means of the more common and simple models based on the widely accepted assumption of cracks developing in pure mode II.

Finally, it is worth highlighting that the proposed model is characterised by a significant level of nonlinearity, which results from the solution of Eq. 4 and Eq. 10, which sometimes results in numerical issues that should be further investigated with the aim to come up with a more robust numerical procedure intended to solve the analysis problem under consideration. This improvement, as well as the formulation of a more systematic identification process for the various parameters required to define the proposed model are among the future developments of the present research.

CITATIONS

Biondini, F.; Frangopol D.M. (2016). "Life-Cycle Performance of Deteriorating Structural Systems under Uncertainty: Review". *ASCE Journal of Structural Engineering*, 142(9), F4016001. https://doi.org/10.1061/(ASCE)ST.1943-541X.0001544.

Breveglieri, M.; Hosseini, A.; Czaderski, C. (2018). *FRP-to-concrete debonding - global and local bond behaviour*. Proceedings of the ninth international conference on fibre-reinforced polymer (FRP) composites in civil engineering (CICE 2018), Paris, France, July 17-19, 2018, 353-360.

Teng, J.G.; Chen, J.F.; Smith, S.T.; Lam L. (2002). FRP: Strengthened RC Structures. Wiley, 272 Pages.

Caballero A., Willam K.J., Carol I. (2008), "Consistent tangent formulation for 3D interface modelling of cracking/fracture in quasi-brittle materials", *Computational Methods in applied mechanics and engineering*, 197: 2804–2822.

Caggiano, A.; Martinelli, E.; Faella, C. (2012). "A fully-analytical approach for modelling the response of FRP plates bonded to a brittle substrate". *International Journal of Solids and Structures*, 49(17):2291-2300. https://doi.org/10.1016/j.ijsolstr.2012.04.029

Carol, I.; Prat, P.C.; López, C.M. (1997). "Normal/Shear Cracking Model: Application to Discrete Crack Analysis". *ASCE Journal of Structural Engineering*, 123(8):765-773. https://doi.org/10.1061/(ASCE)0733-9399(1997)123:8(765).

Czaderski, C.; Motavalli, M. (2007). "40-Year-old full-scale concrete bridge girder strengthened with prestressed CFRP plates anchored using gradient method". *Composites Part B: Engineering*, 38(7-8):878-86. https://doi.org/10.1016/j.compositesb.2006.11.003.

De Lorenzis, L.; Zavarise, G. (2008), "Modeling of mixed-mode debonding in the peel test applied to superficial reinforcements". *International Journal of Solids and Structures*, 45(20):5419-5436. https://doi.org/10.1016/j.ijsolstr.2008.05.024

Martinelli, E.; Czaderski, C.; Motavalli, M. (2011). "Modeling in-plane and out-of-plane displacement fields in pull-off tests on FRP strips". *Engineering Structures*, 33(12):3715-3725. https://doi.org/10.1016/j.engstruct.2011.08.008.

Martinelli, E. (2021). "Closed-form solution procedure for simulating debonding in FRP strips glued to a generic substrate material". *Fibers*. 9(4), 22; https://doi.org/10.3390/fib9040022.

Meier, U.; Brönnimann, R.; Anderegg, P.; Terrasi, G.P.; Motavalli, M.; Czaderski, C. (2016). *Carbon fiber reinforced composites proved to be very successful in construction during a quarter of a century*. Proceedings of ECCM17 – 17th European Conference on Composite Materials, Munich, Germany; 26-30 June 2016: European Conference on Composite Materials, ECCM; https://www.dora.lib4ri.ch/empa/islandora/object/empa:11805.

Moshiri, N.; Martinelli, E.; Czaderski, C.; Mostofinejad, D., Hosseini, A.; Motavalli, M. (2023). "Bond Behavior of Prestressed CFRP Strips-to-Concrete Joints Using the EBROG Method: Experimental and Analytical Evaluation". *ASCE Journal of Composites for Construction*, 27(1). https://doi.org/10.1061/JCCOF2.CCENG-3851.

Roberts, T.M. (1989), "Approximate analysis of shear and normal stress concentrations in the adhesive layer of plated RC beams". *The Struct Engineer*, 67(12):229-233.

The MathWorks Inc. (2022). MATLAB version: 9.13.0 (R2022b), Natick, Massachusetts: The MathWorks Inc. https://www.mathworks.com

ACKNOWLEDGEMENT

Financial contribution of Innosuisse – Swiss Innovation Agency for experimental tests in the framework of project No. 37516.1 IP-ENG is greatly acknowledged. The Authors wish to acknowledge the financial contribution of Swiss National Science Foundation supporting Dr. Martinelli's residence at the Structural Engineering Laboratory of Empa, as part of the Scientific Exchange Programme (IZSEZ0_202268/1). The Authors also sincerely thank S&P Clever Reinforcement Company AG, Switzerland for providing the materials and technical support at the Structural Engineering Research Laboratory of Empa. Finally, the first author wishes to acknowledge the financial support the EU as part of the BEST Project (HE-MSCE-SE, n.101086440).

CONFLICT OF INTEREST

The authors declare that they have no conflicts of interest associated with the work presented in this paper.

DATA AVAILABILITY

Data on which this paper is based is available from the authors upon reasonable request.